applied sciences

MDPI

Article

The Quantification and Evolution of Particle Characteristics of Saturated Silt under Freeze–Thaw Cycles

Jie Zhou [1,*], Zeyao Li [1] and Wansheng Pei [2]

[1] Department of Geotechnical Engineering, Tongji University, Shanghai 200092, China
[2] State Key Laboratory of Frozen Soil Engineering, Northwest Institute of Eco-Environment and Resources, Chinese Academy of Sciences, Lanzhou 730099, China
* Correspondence: zhoujie1001@tongji.edu.cn; Tel.: +86-13636651710; Fax: +86-021-65987079

Abstract: Freeze–thaw action is a complicated process. How it affects particle characteristics of saturated silt may provide a much clearer understanding of its internal mechanism. A series of specific apparatus were developed for sample reconstitution, including sand pluviation device, freeze–thaw device, and special sampling device. After reconstituting samples by sand pluviation method and a specific parameter-controlled freeze–thaw testing, scanning electron microscope (SEM) and laser scattering and transmissometry (LST) tests were conducted to explore the particle characteristics of silt under freeze–thaw cycles. The test results show that freeze–thaw action could probably induce the particles' (60–200 μm) breakage, also affecting the clay particles' (less than 5 μm) aggregation. With the increase of freeze–thaw times, freeze–thaw action on the particle impact decreases. The larger the effective confining pressure, the lower the freezing temperature, greater the compaction degree, and higher the fine content, which can all aggravate the effects of freeze–thaw action on silt particles. Finally, two characteristic evolution modes of particle structure under freeze–thaw cycles have been inferred based on particle interaction during the freeze–thaw process, which could provide a reference for long-term durability evaluation of pavements in cold regions.

Keywords: freeze–thaw cycle; scanning electron microscope (SEM) and laser scattering and transmissometry (LST); saturated silt; particle crushing and aggregating; particle characteristic index

Citation: Zhou, J.; Li, Z.; Pei, W. The Quantification and Evolution of Particle Characteristics of Saturated Silt under Freeze–Thaw Cycles. *Appl. Sci.* **2022**, *12*, 10703. https://doi.org/10.3390/app122110703

Academic Editor: Daniel Dias

Received: 5 September 2022
Accepted: 9 October 2022
Published: 22 October 2022

1. Introduction

Cohesionless soil is widely distributed in the middle and lower reaches of rivers, such as silt. They are typical frost-susceptible soils, which have a significant silt/fine content allowing the additional water rise of capillary during freezing. This water can turn to ice lenses in winter and further water is drawn up from frozen front to balance the capillary forces. This cycle ultimately leads to heaving at the surface which causes pavement cracking and uplifting (Figure 1).

It is further complicated as the upper ice thaws in summer. The volume of water held as ice is many times greater than water held by the soil under saturated conditions (due to moisture migration). The water cannot drain down through the soil as it is still frozen. The result is a further weakening of the highway as the subgrade's ground-bearing capacity is diminished. Even though freeze–thaw action is a complicated multi-field multi-scale process, the inherent cause of this bearing weakening can be traced to the particle variation characteristics of saturated cohesionless soil deposited in water environment, such as particle breakage, rearrangement, and rounding, by freeze–thaw cycles.

So far, the effects of freeze–thaw action on saturated cohesionless soil particles have been studied over several decades. Arturo [1,2] conducted horizontal and vertical freezing experiments on gravel soil. The test results showed that the freeze–thaw action could cause a certain sorting phenomenon. Freeze–thaw action would cause large particles to move against freezing direction, and small particles to move in freezing direction. Edwin and

Anthony [3] studied the freeze–thaw characteristics of cohesionless soils. These results showed that freezing and thawing can change the pore structure of the soil, thereby increasing the permeability of the soil. Konrad [4] conducted the freeze–thaw cycle test on saturated clayey silt, and qualitatively analyzed the structural characteristics of the freeze–thaw soil, concluding that freeze–thaw cycles could destroy the bonding force between soil particles and induce particle rearrangement. Qi et al. [5] used SEM to quantitatively study the microscopic pore characteristics of silt soil in upper reaches of the Yellow River under freeze–thaw cycle. The results showed that the freeze–thaw cycle can make small pores smaller and large pores larger. Mu et al. [6] scanned the loess with open system freeze–thaw by electron microscope, and quantitatively analyzed its pore characteristics, obtaining the process and mechanism of the effects of freeze–thaw cycles on pore structures. Tan et al. [7] analyzed the effects of freeze–thaw on saturated silt pore microstructure using nitrogen adsorption and mercury injection. These results showed that freeze–thaw cycles have little effect on pores with diameters less than 10^{-8} m, whilst having great influence on 10^{-8}–10^{-4} m pores. Tang and Li [8] studied the pore structure characteristics of saturated freeze–thaw silt and silt through scanning electron microscope and mercury intrusion test. The results showed the accumulated pore volume and pore area of frozen–thawed silty sand increased along with decreasing freezing temperature; the most probable pore size and probability decrease along with increasing freezing temperature. Jin et al. [9] analyzed the dynamic structure characteristics of salty silt under freeze–thaw cycles. Zheng et al. [10] qualitatively investigated the particle gradation and pore characteristics of the Yellow River flooded area under freeze–thaw cycle using nuclear magnetic resonance. Ren and Vanapalli [11] measured the SFCC (including both freezing and thawing branches) of two kinds of cohesionless soil for different freeze–thaw cycles and analyzed the effect of freeze–thaw cycles on soil texture. The results show that the effect of freeze–thaw on soil texture is mainly the production of lens. Leuther and Schlüter [12] analyzed the impact of freeze–thaw cycles on soil structure and soil hydraulic properties, concluding that freeze–thaw has a greater impact on soil pores and can increase soil permeability. The effects of initial freeze–thaw are most obvious. Zhou et al. [13] conducted mercury intrusion experiments on saturated artificial frozen–thawed silty sand deposited in middle and lower reaches of the Yangtze River and obtained the influence of freeze–thaw action on the pore characteristics of Nanjing saturated silt fine sand. The results showed that freezing and thawing could loosen the silty fine sand structure and increase the soil average.

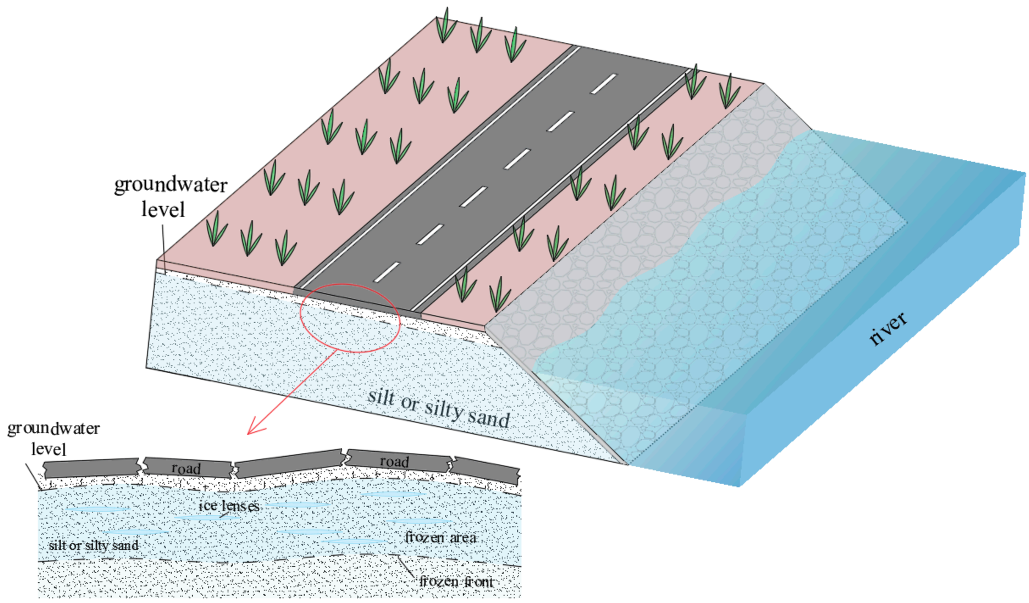

Figure 1. Pavement damage during freeze–thaw cycles in saturated cohesionless soil.

It can be seen that research about the effects of freeze–thaw action on cohesionless soil has mainly concentrated on macrostructure and pore characteristics. However, there are relatively few studies to quantitatively evaluate the effects of freeze–thaw action on the particle characteristics of cohesionless soil with fine particles, especially combined with other impact factors, such as confining pressure, compaction degree, etc.

The particle characteristics directly affect the macro-physical and mechanical properties of soil. Studying the effects of freeze–thaw action on the particle characteristics of saturated cohesionless soil deposited in water environment can therefore help us to understand the freeze–thaw mechanism on the physical and mechanical properties of soil, especially when multiple impact factors are involved, so as to assist traffic engineering construction along rivers in cold regions or artificial ground freezing to ensure engineering safety. Hence, after reconstituting samples by sand pluviation method and a specific parameter-controlled freeze–thaw testing, scanning electron microscope (SEM) test and the laser scattering and transmissometry (LST) were conducted for silt before and after freeze–thaw cycles, to explore the effects of freeze–thaw action on the particle characteristics of saturated silt deposited in water environments.

2. Test Materials

Saturated cohesionless soil is widely distributed in the Yangtze River coastal area. The cohesionless soil layers deposited in river facies such as silt and silty sand (less fine) are important soil layers for urban engineering construction. This paper focuses on the third layer (mezzanine) of silt near the Shangyuanmen subway station of Nanjing Metro Line 3$^{\#}$ along the Yangtze River. In this research area, groundwater level is high, and the soil layers are saturated. The main component of soil particles is silicate minerals, and the soils are anisotropic in orientation. Through geotechnical investigation of Shangyuanmen subway station of Nanjing Metro Line 3$^{\#}$, the particle shape characteristics of Nanjing saturated silt are shown in Figure 2; the particle grading curves are shown in Figure 3. The basic physical parameters are shown in Table 1:

Figure 2. The shape of soil particles of saturated silt along Yangtze River.

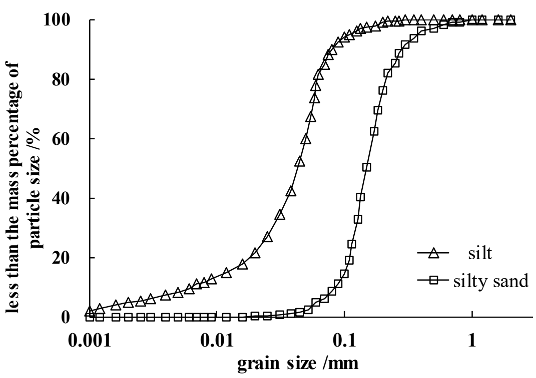

Figure 3. Soil particle grading curves (a. silt; b. silty sand).

Table 1. Physical and mechanical properties of soils.

	Water Content/ %	Unit Weight/ (kN/m^3)	Natural Void Ratio	Particles Specific Gravity	Maximum Void Ratio	Minimum Void Ratio	Cohesion/ kPa	Internal Friction Angle/°	Compression Modulus/ kPa	Uniformity Coefficient	Fine Particle Content/%
silt	27.3	18.9	0.797	2.69	1.31	0.69	7.2 *	28.1 *	10.27	6.09	88.3
silty sand	24.8	19.4	0.734	2.70	1.18	0.65	5.3 *	30.6 *	10.82	1.89	7.2

Note: * is obtained by direct shear test.

3. Experimental Program

To ensure the orientation of sample particles, the sand pluviation method is used for sample reconstitution by taking compaction degrees, fine contents, etc., into account; then, the reconstituted samples were frozen and thawed under different confining pressures and freezing temperatures; finally, scanning electron microscope (SEM) and laser scattering and transmissometry (LST) tests were both conducted to comprehensively explore the particle characteristics of saturated silt under long-term freeze–thaw cycles. The testing procedures were as follows:

① Firstly, dry and smash the undisturbed soil into soil particles, and pass it through 2.0 mm fine sieve for particle separation;
② Use the sample preparation device of sand pluviation method (as shown in Figure 4) for sample preparation:

The sample preparation device consists of a sand-spreading device, a water tank, a movable trolley platform, and some double valves. The water level of water tank is 1 m higher than the double valves [13]. To avoid sorting due to different particle diameters during the initial spreading period, a movable trolley platform is specially set up. After sand spreading for a period of time (30 s) move the trolley platform to the sand accumulation area to accumulate sand. The compactness degree of sand samples could be controlled initially by falling distance and falling amount, and then accurately controlled by sample compactor. The length and diameter of sand samples are 80.0 mm and 39.1 mm, respectively.

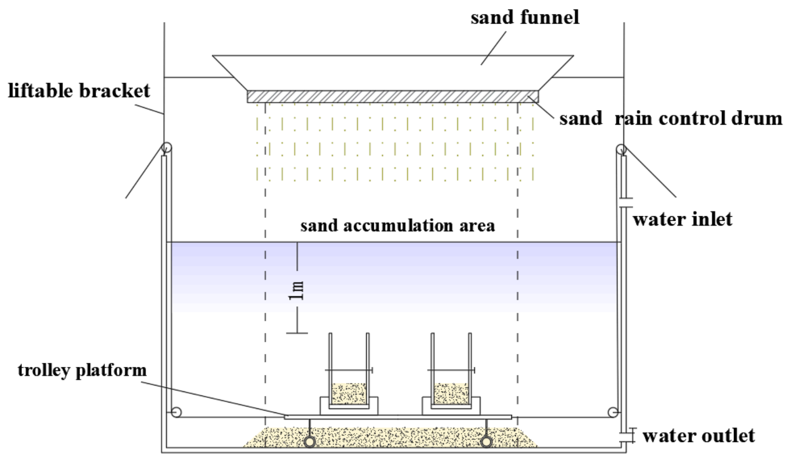

Figure 4. Sample preparation device of sand pluviation method for soil reconstitution.

③ Store the reconstituted samples in a vacuum saturator to saturate for 12 h;
④ Place the saturated samples on the freeze–thaw device (as shown in Figure 5) and set the preloading:

First, place the saturated samples on the freeze–thaw device. Open the drainage channel of freeze–thaw device and put an appropriate amount of weight on loading frame according to the effective confining pressure of the experimental program. Close the drainage channel after loading for 2 h. Then add another appropriate amount of weight to make the loading reach the designed total overburden stress value.

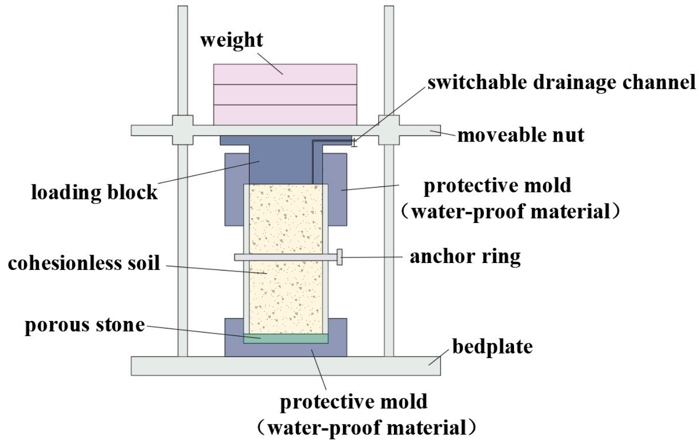

Figure 5. Freeze–thaw device diagram.

⑤ Put the freeze–thaw device with sample under a certain confining pressure of weights into a DW-40 type low temperature test chamber and freeze for 12 h. The freezing temperature matches the experimental program. After freezing, take it out to room temperature (constant temperature 20 °C by air conditioner) and thaw for 12 h. In this way, cycle the freeze–thaw operation until the design freeze–thaw cycles are reached.

⑥ Make the SEM sample and observe its microstructure:

The soil structure of silt can hardly be preserved without special device and techniques. In this paper a special SEM sampling device and a kind of curing agent, menthol, are used for SEM sample preparation. Evenly press the SEM sampling device by using a pallet into the soil sample. The SEM sampling device is 10 mm diameter, 5 mm height, and 0.1 mm thickness by No. 400 filter mesh (0.038 mm), as shown in Figure 6. Heat menthol to melt, then sprinkle the liquid menthol evenly on the surface of soil sample through the filer mesh with a small sprinkling can. After the menthol solidifies, it preserves the soil structure of silt at best. Set the soil sample into the sample chamber of SEM, start vacuum pump to sublimate the solid menthol, then run the SEM and take clear SEM images.

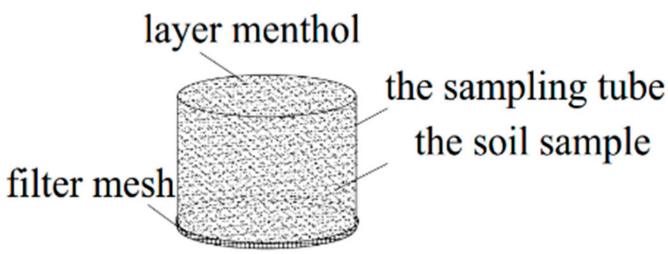

Figure 6. The sampling device of SEM.

⑦ Use LST to further determine the particle characteristics of soil:

Weigh 2 g of the dried frozen–thawed soil sample and put it into a 500 mL beaker with 200 mL distilled water. After soaking overnight, add 5 mL of 4% sodium hexametaphosphate, then add distilled water to 500 mL. Turn on the magnetic stirrer until the particles in suspension are evenly distributed. Finally, use the LST to determine the particle characteristics of the suspension.

The depth of natural frozen soil in Nanjing area is generally less than 1 m, and the depth of artificial frozen soil is about 7–15 m when using artificial ground freezing to construct the subway cross passages [13]. There are two test groups: the silt test group (A0–A16) and the prepared soil with less fine (from silty sand to silt) test group (C1–C4). The silt test group sets vertical confining pressure of 150 kPa, effective confining pressure of 75 kPa (the buried depth is about 7.8 m), relative bulk density of 0.827, freeze–thaw cycles of 20 times, fine particle content of 88.3% as the basic test conditions for comparison according to field conditions. The whole experimental program is designed to explore the effects of freeze–thaw cycles (N), effective confining pressure (σ), freezing temperature (T), compaction degree (D_r), and fine particle content (L) on the particle characteristics of cohesionless soil deposited in water environments (shown as Table 2).

Table 2. Experimental program.

Sample Label	Soil Type	Freeze–Thaw Cycles	Simulation Depth/m	Vertical Confining Pressure & Effective Confining Pressure/kPa	Freezing Temperature/°C	Compaction Degree	Fine Particle Content/%	Remark
A0	silt	0	7.8	150&75	/	0.827	88.3	
A1	silt	10	7.8	150&75	−20	0.827	88.3	
A2	silt	20	7.8	150&75	−20	0.827	88.3	Basic test
A3	silt	30	7.8	150&75	−20	0.827	88.3	
A4	silt	50	7.8	150&75	−20	0.827	88.3	
A5	silt	100	7.8	150&75	−20	0.827	88.3	
A6	silt	20	0.0	0&0.0	−20	0.827	88.3	
A7	silt	20	3.8	75&37.5	−20	0.827	88.3	
A8	silt	20	11.6	225&112.5	−20	0.827	88.3	
A9	silt	20	15.4	250&125	−20	0.827	88.3	
A10	silt	20	7.8	150&75	−20	0.300	88.3	
A11	silt	20	7.8	150&75	−20	0.500	88.3	
A12	silt	20	7.8	150&75	−20	0.700	88.3	
A13	silt	20	7.8	150&75	−20	0.900	88.3	
A14	silt	50	7.8	150&75	−5	0.827	88.3	
A15	silt	50	7.8	150&75	−10	0.827	88.3	
A16	silt	100	7.8	150&75	−30	0.827	88.3	
C1	prepared soil	20	7.8	150&75	−20	0.830	23.4	Silty sand
C2	prepared soil	20	7.8	150&75	−20	0.833	39.6	Silty sand
C3	prepared soil	20	7.8	150&75	−20	0.836	55.9	Silt
C4	prepared soil	20	7.8	150&75	−20	0.839	72.1	Silt

4. Test Results

4.1. Qualitative Analysis of Particle Structure of Silt under Freeze–Thaw Cycles by SEM

The microscopic particle structures of saturated silt deposited in water environments (scanning magnification of electron microscope 500 times) with different freeze–thaw cycles are shown in Figure 7.

It can be seen from Figure 7 that the unfrozen silt is mainly composed of irregular sand particles and silt particles, and a small amount of clay particles is randomly distributed. The soil particles have a certain orientation; the flaky soil particles are arranged in the horizontal direction and form relatively stable staggered structure. Compared with unfrozen silt, the fine content of silt after freeze–thaw is significantly increased, irregular flocs are formed, and the orientation characteristic of soil particles is weakened. The more freeze–thaw cycles the silt experienced, the more fine flakes (aggregation) the silt contains, more irregular flocculent content and less obvious particles orientation the soil has. This shows that freeze–thaw action can cause main particles' breakage and some fine aggregation, generate irregular flocs, and weaken the orientation of particles on silt. It should be noted that long-term freeze–thaw cycles can not only induce particle crushing and maybe some fine aggregate, but also affect the particle shapes, resulting in less regular orientations.

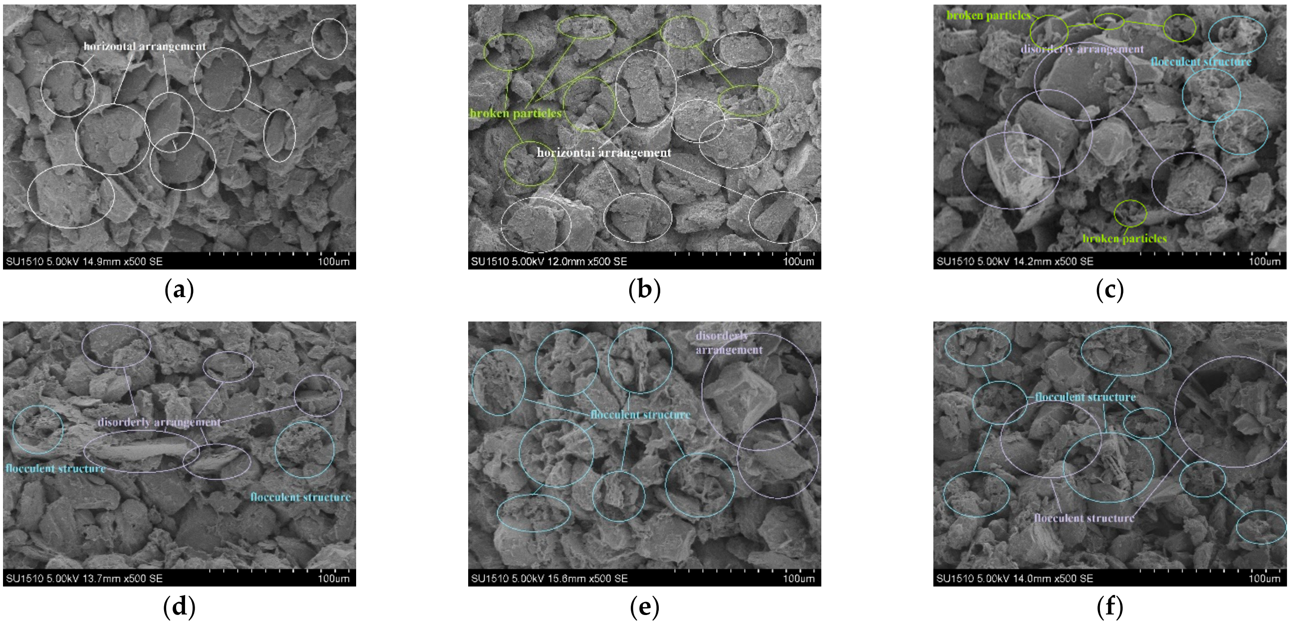

Figure 7. The SEM images of silt under different freeze–thaw cycles. (**a**) Unfrozen; (**b**) freeze–thaw 10 times; (**c**) freeze–thaw 20 times; (**d**) freeze–thaw 30 times; (**e**) freeze–thaw 50 times; (**f**) freeze–thaw 100 times.

4.2. Quantitative Analysis of Particle Structure of Silt under Freeze–Thaw Cycles by LST

4.2.1. Particle Characteristic Evaluation Parameters Establishment

The particle characteristics of soil could be further measured by LST. Under the condition of vertical confining pressure 150 kPa, effective confining pressure 75 kPa, freezing temperature −20 °C, and relative bulk density 0.827, the particle bulk density curves of silt with different freeze–thaw cycles are shown in Figure 8. It can be seen that as the silt experienced more freeze–thaw cycles, the content of clay particles smaller than 5 µm is reduced; the content of 5–10 µm particles changes in a stable fluctuating state; the content of 5–50 µm particles increases significantly; the content of 50–60 µm particles remains basically unchanged; the content of 60–200 µm particles decreases; the content of particles larger than 200 µm does not change significantly. Combined with the SEM images of silt under long-term freeze–thaw cycles (Figure 7), it can see that the freeze–thaw action probably induces the clay particles (less than 5 µm) to aggregate and form flocculent structure; probably inducing the part silt and sand particles (60–200 µm) in breakage. The diameters of formed flocculent structures (aggregated) and broken particles are distributed from 5–60 µm.

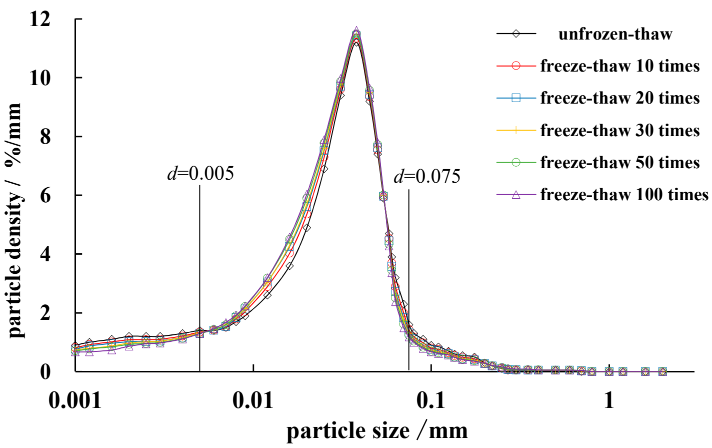

Figure 8. The particle bulk density curves of silt.

As early as 1985, Hardin [14] defined a parameter crushing index B_r to evaluate the particle size variation in soil shearing. It took the area enclosed by d = 0.074 mm, P = 100% (P is the percentage content of particles less than a certain size (%), d is the soil particle size (mm)), and the gradation curve before particle breakage in P-lg$d$ coordinate system as the crushing potential S_p, and the reduced area of gradation curve after testing was taken as the particle crushing amount S, and the two were divided to obtain the crushing index B_r.

$$B_r = S/S_p \tag{1}$$

The model is mainly aimed at particle breakage size greater than 0.074 mm of sand particles [15,16] (he regarded that the shear failure of soil could not affect particles below 0.074 mm [10,17]). However, in our research, the fine particles of soil account for 88.3%. As shown in the SEM images (Figure 7) and preliminary analysis of Figure 8, for silt under long-term freeze–thaw cycles, the soil particles were main influenced at a range of 1–2000 μm and soil particles both could break and aggregate in 5–60 μm, so a particle size index B_f of silt is defined in this paper to describe the total particle size variation characteristics of silt under long-term freeze–thaw cycles:

$$B_f = (|\,\mathrm{S1}\,| + |\,\mathrm{S2}\,|)/S_p \tag{2}$$

where S is the amount of particle size variation (%•mm), which is characterized by the area between the particle accumulation curve of silt before and after freeze–thaw cycles in P-lg$d$ coordinate system (note: this area is the sum of the variation amount including particles aggregation |S1| and particles breakage |S2|. Shown in Figure 9); S_p is the variation potential (%•mm), which is characterized by the area along with d = 0.001 mm, P = 100%, and particle accumulation curve in P-lg$d$ coordinate system.

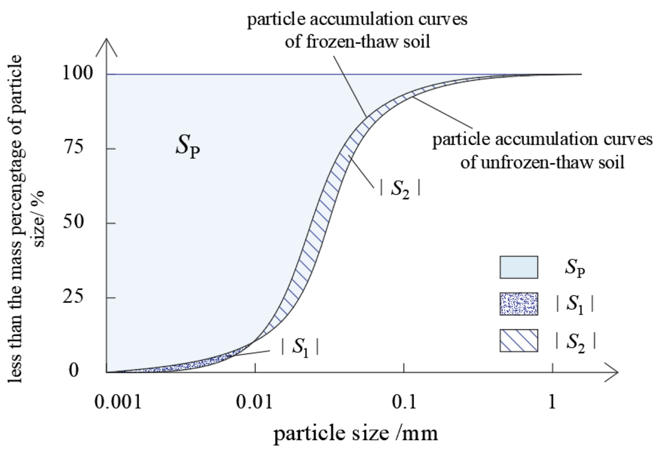

Figure 9. Schematic diagram of total particle size variation index.

From SEM image observing (Figure 7) and preliminary analysis of LST (Figure 8), freeze–thaw cycles not only change particle size, but also affect particle shape. Analogously, the concept of sphericity potential is proposed in this paper. The variation degree of total particle shape is characterized by the ratio of sphericity variation amount to sphericity potential.

The total particle shape index B_s of silt could be defined to describe the particle shape variation characteristics under long-term freeze–thaw cycles:

$$B_s = Q/Q_p \tag{3}$$

where Q is the amount of particle sphericity variation (mm), which is characterized by the area between the sphericity curve of silt before and after freeze–thaw cycles in S_s-lg$d$ coordinate system, shown in Figure 10; Q_p is the particle sphericity potential (mm), which is characterized by the area along with d = 0.001 mm, S_s = 1, and sphericity curve of silt before freeze–thaw in S_s-lg$d$ coordinate system; S_s is the sphericity of soil particles [4]:

$$S_s = \frac{P_{epqc}}{P_{real}} = 2\sqrt{\pi \cdot A} / p_{real} \tag{4}$$

where S_s is between 0 and 1. The smaller the S_s, the more irregular the soil particle shape; P_{epqc} is the perimeter of equivalent projection circle measured by LST (m); P_{real} is the actual boundary perimeter of particle projected image (m); A is the projected area of particle (m).

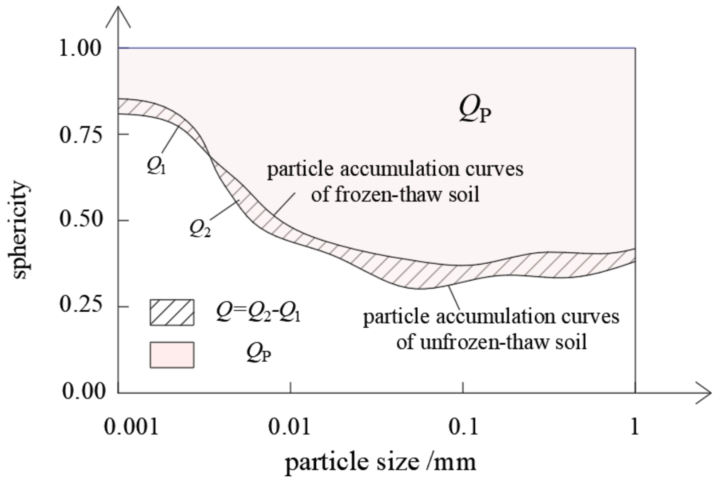

Figure 10. Schematic diagram of total particle shape variation rate.

Under the condition of vertical confining pressure 150 kPa, effective confining pressure 75 kPa, freezing temperature −20 °C, and relative bulk density 0.827, the sphericity curves of silt with different freeze–thaw cycles are shown in Figure 11. It shows that the sphericity of silt ranges from 0.46–0.90, and the shapes of small particles are characterized by roundness, while the shapes of large particles are relatively poor. The sphericity of particles smaller than 40 µm with different freeze–thaw cycles hardly change; that means freeze–thaw action has no obvious effect on the shape of particles smaller than 40 µm in silt. For particles larger than 40 µm, freeze–thaw action could cause a certain statistical increase of sphericity, especially the sphericity of particles larger than 100 µm, which show more statistically significant increases.

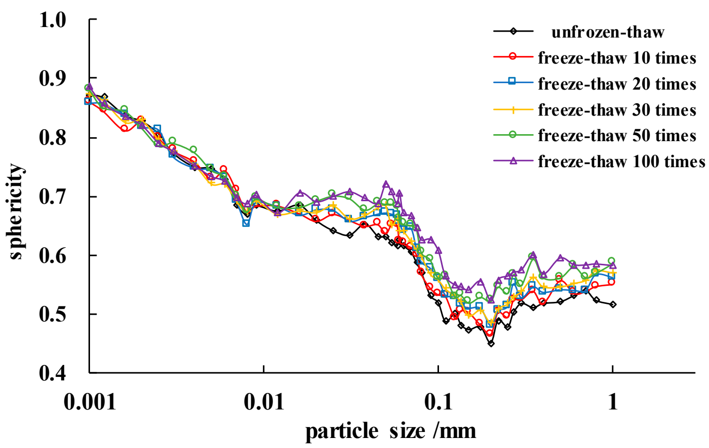

Figure 11. The sphericity curves of silt.

4.2.2. The Particle Characteristics of Silt under Freeze–Thaw Cycles

Under the condition of vertical confining pressure 150 kPa, effective confining pressure 75 kPa, freezing temperature −20 °C, and relative bulk density 0.827, the values of B_f of silt with different freeze–thaw cycles are shown in Figure 12. It shows that total particle size index increases with freeze–thaw cycles. The initial freeze–thaw cycles have a greater degree of influence on total particle size index. With the more freeze–thaw cycles the silt has experienced, the influence degree of single freeze–thaw cycle on the particle size becomes smaller.

To quantitatively describe the effects of freeze–thaw action on the total particle size index, a hyperbolic type total particle size variation model is established under freeze–thaw cycle number:

$$B_f = \frac{N^a}{b + cN^a} \tag{5}$$

where a, b, c are model parameters, which respectively relate to accumulative total particle size index, total particle size index in the first freeze–thaw cycle, and the final total particle size index.

A hyperbolic type total particle size variation model was used to fit the relationship between total particle size index of silt and freeze–thaw cycles (show as Equation (6)), and the data fits well with the correlation coefficient R^2 value of 0.98.

$$B_f = \frac{N^{0.973}}{1.113 + 0.056N^{0.973}} R^2 = 0.98 \tag{6}$$

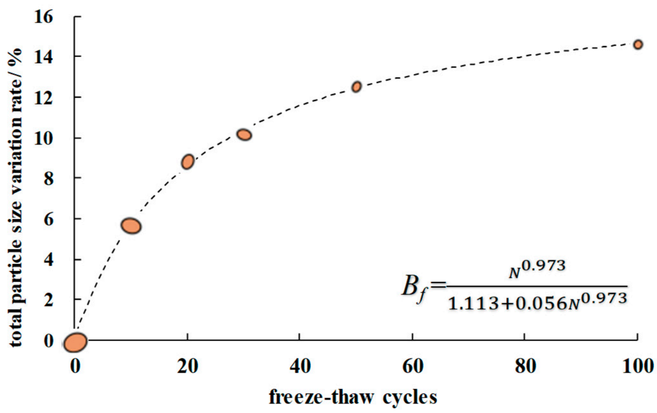

Figure 12. The effect of freeze–thaw cycles on the total particle size of silt.

Under the condition of vertical confining pressure 150 kPa, effective confining pressure 75 kPa, freezing temperature −20 °C, and relative bulk density 0.827, the total particle shape index values of silt with different freeze–thaw cycles are shown in Figure 13. It shows that the total particle shape index increases with freeze–thaw cycles. This means that freeze–thaw action causes the total particle shape of silt to become more spherical. The initial freeze–thaw cycles have a greater degree of influence on total particle shape index. With more freeze–thaw cycles, the influence degree of a single freeze–thaw cycle on the particle shape of silt becomes smaller and smaller.

Similarly, a hyperbolic type model is established to describe the effects of freeze–thaw cycles on total particle shape index of silt:

$$B_s = \frac{N^d}{e + fN^d} \tag{7}$$

where d, e, f are model parameters, which are respectively related to accumulative growth rate of total particle shape variation, total particle shape index in the first freeze–thaw cycle, and the final total particle shape index.

A hyperbolic type total particle shape variation model was used to fit the relationship between total particle shape index of silt and freeze–thaw cycles (shown as Equation (8)), and the data fit relatively well with the correlation coefficient R^2 value of 0.97.

$$B_s = \frac{N^{1.249}}{10.45 + 0.091N^{1.249}} R^2 = 0.97 \tag{8}$$

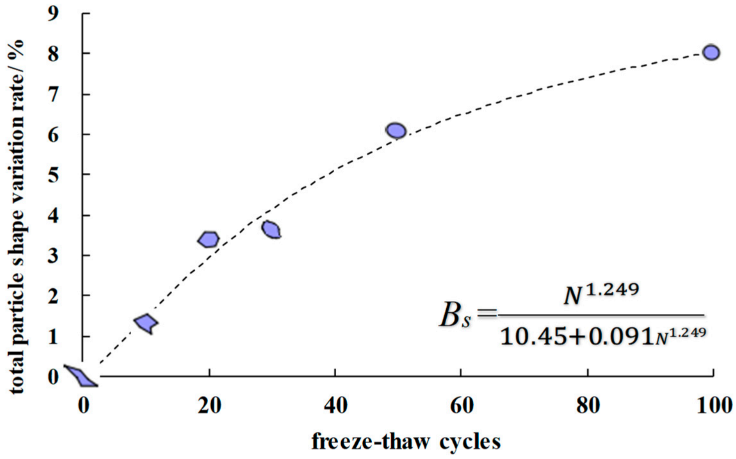

Figure 13. The effect of freeze–thaw cycles on the total particle shape of silt.

4.3. Particle Characteristics of Freeze–Thaw Effect under Different Impact Factors

4.3.1. Confining Pressure

Under the conditions of freeze–thaw cycles 20, freezing temperature −20 °C, and relative bulk density 0.827, the total particle size index values of silt with different freeze–thaw cycles are shown in Figure 14. It shows that within the depth range of natural frozen soil and artificial frozen soil, the greater the effective confining pressure, the higher the total particle size index of silt. With the higher effective confining pressure, the influence degree of effective confining pressure on total particles size is smaller and smaller. The quadratic function model is used to fit the relationship between total particle size index of silt and effective confining pressure (shown as Equation (8)), and the data fitting effect is relatively good.

$$B_f = -3.1 \times 10^{-4}\sigma^2 + 0.0896\sigma + 3.813 R^2 = 0.99 \tag{9}$$

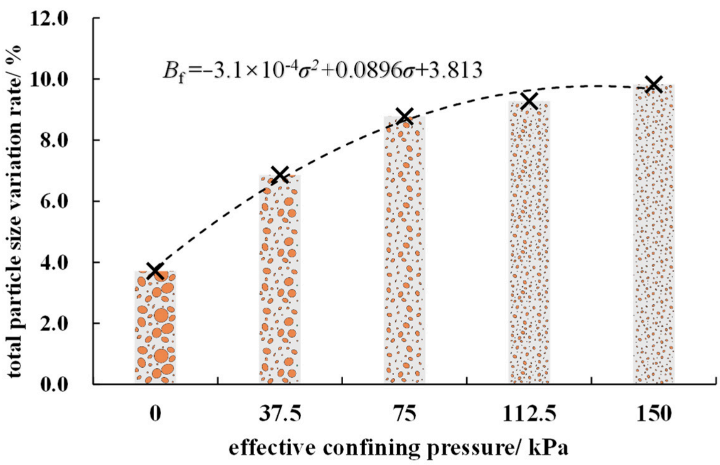

Figure 14. The effect of effective confining pressure on the total particle size of silt.

Under the conditions of freeze–thaw cycles 20, freezing temperature −20 °C, and relative bulk density 0.827, the total particle shape index values of silt with different freeze–thaw cycles are shown in Figure 15. It shows that within the depth range of natural frozen soil and artificial frozen soil, the greater the effective confining pressure, the higher the total particle shape index of silt. With higher effective confining pressure, the variation of effective confining pressure has less and less influence degree on total particle shape. The quadratic function model is used to fit the relationship between total particle shape index of silt and effective confining pressure (shown as Equation (9)), and the data fitting effect is relatively good.

$$B_s = -6.1 \times 10^{-5}\sigma^2 + 0.0198\sigma + 2.248R^2 = 0.99 \quad (10)$$

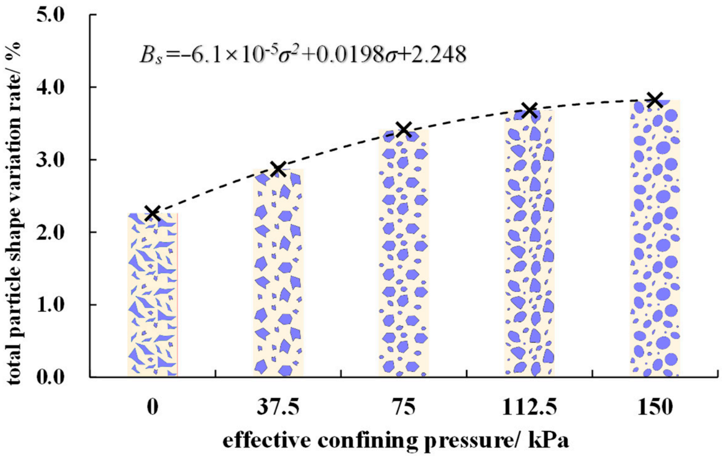

Figure 15. The effect of effective confining pressure on the total particle shape of silt.

4.3.2. Freezing Temperature

Under the condition of vertical confining pressure 150 kPa, effective confining pressure 75 kPa, and relative bulk density 0.827, the total particle size index values of silt with 20 freeze–thaw cycles at different temperatures are shown in Figure 16. It shows that within the temperature range of natural frozen soil and artificial frozen soil, the freezing temperature and the total particle size index of silt are roughly linearly correlated. The total particle size index of silt linearly increases with the decrease of freezing temperature. Linear fitting is performed on total particle size index of silt and freezing temperature (shown as Equation (11)), and the data fitting effect is relatively good.

$$B_f = -0.150T + 5.768 \quad R^2 = 0.98 \quad (11)$$

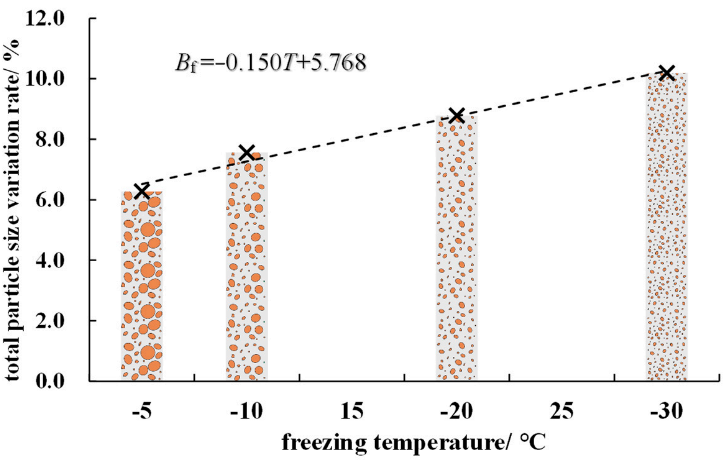

Figure 16. The effect of freezing temperature on the total particle size of silt.

Under the condition of vertical confining pressure 150 kPa, effective confining pressure 75 kPa, and relative bulk density 0.827, the total particle shape index values of silt with 20 freeze–thaw cycles at different temperatures are shown in Figure 17. The freezing temperature and total particle shape index are roughly linearly correlated. The lower the freezing temperature, the higher the total particle shape index. Linear fitting is performed on total particle shape index of silt and freezing temperature (shown as Equation (12)), and the data fitting effect is relatively good.

$$B_s = -3.3 \times 10^{-2}T + 2.713 \quad R^2 = 0.98 \tag{12}$$

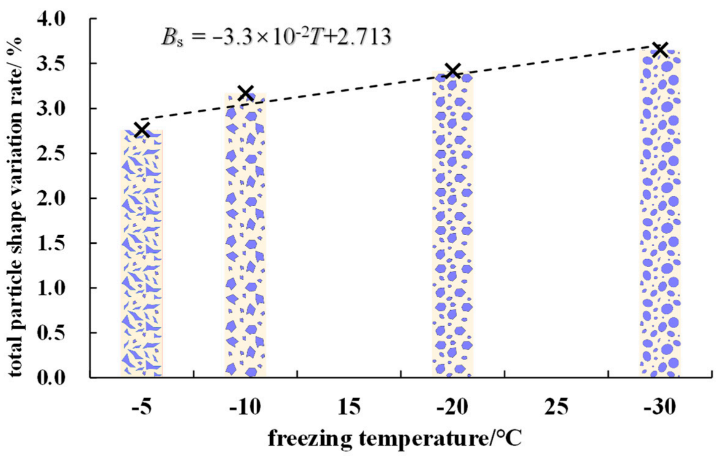

Figure 17. The effect of freezing temperature on the total particle shape of silt.

4.3.3. Compaction Degree

Figure 18 shows the total particle size index values of silt with different densities under the conditions of vertical confining pressure 125 kPa, effective confining pressure 75 kPa, and freezing temperature −20 °C after 20 freeze–thaw cycles. It can be seen from Figure 17 that the silt with higher relative bulk density would have higher total particle size index. The higher the relative bulk density, the smaller the influence degree of relative bulk density changing on total particles size. The quadratic function model is used to fit the relationship between total particle size index of silt and relative bulk density (shown as Equation (13)), and the data fitting effect is relatively good.

$$B_f = -9.25{D_r}^2 + 16.96D_r + 1.160 \quad R^2 = 0.98 \tag{13}$$

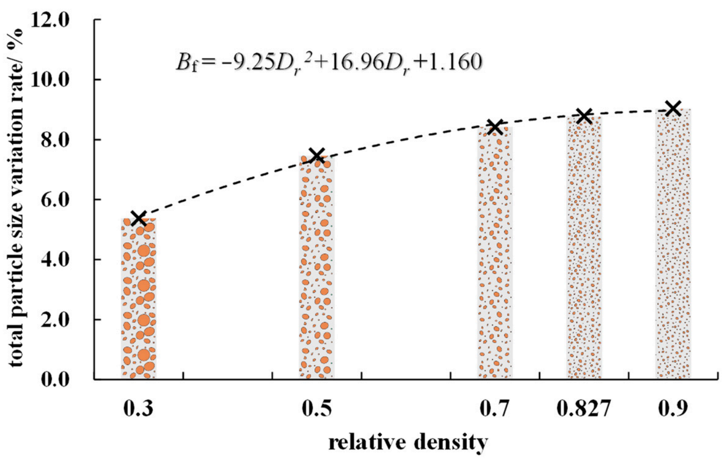

Figure 18. The effect of soil bulk density on the total particle size of silt.

Figure 19 shows the total particle shape index values of freeze–thaw silt with different densities under the conditions of vertical confining pressure 150 kPa, effective confining pressure 75 kPa, and freezing temperature −20 °C after 20 freeze–thaw cycles. It shows that the higher the relative bulk density, the higher the total particle shape index of silt. With the increase of relative bulk density, the variation of relative bulk density has less and less influence on total particle shape. The quadratic function model is used to fit the relationship between total particle shape index of silt and relative bulk density (shown as Equation (14)), and the data fitting effect is relatively good.

$$B_s = -1.66{D_r}^2 + 3.04D_r + 2.029 \quad R^2 = 0.98 \tag{14}$$

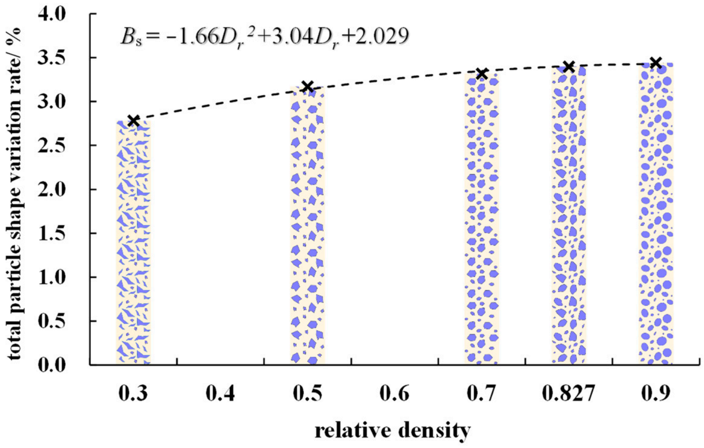

Figure 19. The effect of soil bulk density on the total particle shape of silt.

4.3.4. Fine Content

By mixing the silt and silty sand for a certain proportion, the cohesionless soil with different fine particle contents would be obtained. Under the condition of −20 °C freezing temperature for 20 freeze–thaw cycles, the total particle size index values of cohesionless soil with different fine particles content are shown in Figure 20. It can be seen that the total particle size index of cohesionless soil with higher fine particles content is greater. As the fine particles content increases, the variation of fine particles content has less and less influence degree on total particle size. The quadratic function model is used to fit the relationship between total particle size index of silty sand and fine particles content (shown as Equation (15)), and the data fitting effect is relatively good.

$$B_f = -1.1 \times 10^{-3} L^2 + 0.195L + 0.1368 \quad R^2 = 0.97 \tag{15}$$

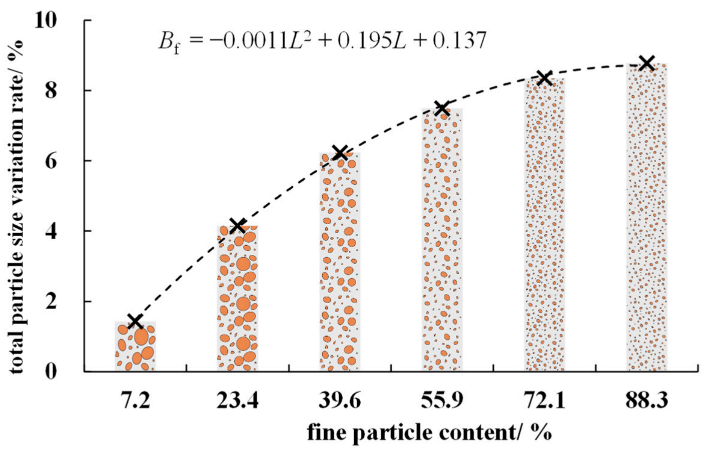

Figure 20. The effect of fine content on the total particle size.

Under the condition of −20 °C freezing temperature for 20 freeze–thaw cycles, the total particle size index values of cohesionless soil with different fine particles content are shown in Figure 21. It shows that the total particle shape index of the freeze–thaw cohesionless soil with higher fine particles content is greater. As the fine particles content increases, the variation of fine particles content has less influence degree on total particle shape. The quadratic function model is used to fit the relationship between total particle shape index and fine particles content (shown as Equation (16)), and the data fitting effect is relatively good.

$$B_s = -4.1 \times 10^{-4} L^2 + 0.078L + 0.182 \quad R^2 = 0.99 \tag{16}$$

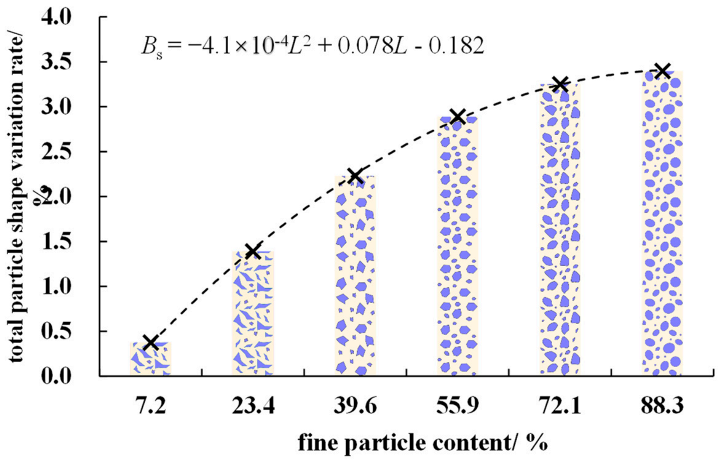

Figure 21. The effect of fine content on the total particle shape.

5. Mechanism and Discussion

When saturated soil is freezing, the phase variation of pore water would cause volume expansion which generates wedge force to increase the distance of soil particles [18]. Due to the capillary force and van der Waals force, the capillary water and film water in soil are less likely to be frozen than gravity water. The smaller the pores, the greater the proportion of capillary water and film water in these pores and the less likely they are to be frozen [19]. This induces the large pores near the freezing front to freeze first. With the continuous expansion of the freezing front, the medium pores and small pores nearby are frozen successively [20].

The soil of silt not only contains a large amount of silt particles (5–75 μm), but also contains some clay particles (<5 μm) and sand particles (>75 μm) (Figure 22a). Clay particles are smaller in size, larger in specific heat capacity, more spherical in shape, and the diameters of their nearby pores are small. Due to the small particle size, small diameter of nearby pores, and large specific heat capacity, pore water surrounding clay particles are less likely to be frozen under the same conditions than silt particles and sand particles. During the freezing process, the wedge force formed by the growth of ice crystals first acts on sand particles and silt particles, causing more frost heave displacements for large and medium particles, and increasing the diameter of nearby pores [21,22]. This exacerbates the possibility of mutual attraction and aggregation for clay particles (Figure 22b). Because of their small diameter and spherical shape of clay particles, the wedge force of ice crystal growth does not easily impact the clay particles themselves, so the shape variations of clay particles are not obvious. Due to the large particle size and irregular shape of silt particles and sand particles, the wedge force of ice crystal growth is more likely to make their structure looser and induces irregular boundary collapse of particles. Hence, it produces the phenomenon of silt particles and sand particles becoming broken, the total particle arrangement becoming messy, and the total particle shape becoming spherical (Figure 22c). Lowering the freezing temperature could cause the wedge force for ice crystal growth to become greater. Increasing the effective confining pressure has the same impact as lowering the freezing temperature. The higher the compaction degree, the greater the friction between soil particles, and soil particles are more likely to break rather than slip. Therefore, greater effective confining pressure, lower freezing temperature, and greater compactness could all exacerbate the impact of freeze–thaw action on total particle size and total particle shape to a certain extent. The result would be that freeze–thaw action has greater effects on total particles characteristics of silt with greater effective confining pressure, lower freezing temperature, and greater compaction degree.

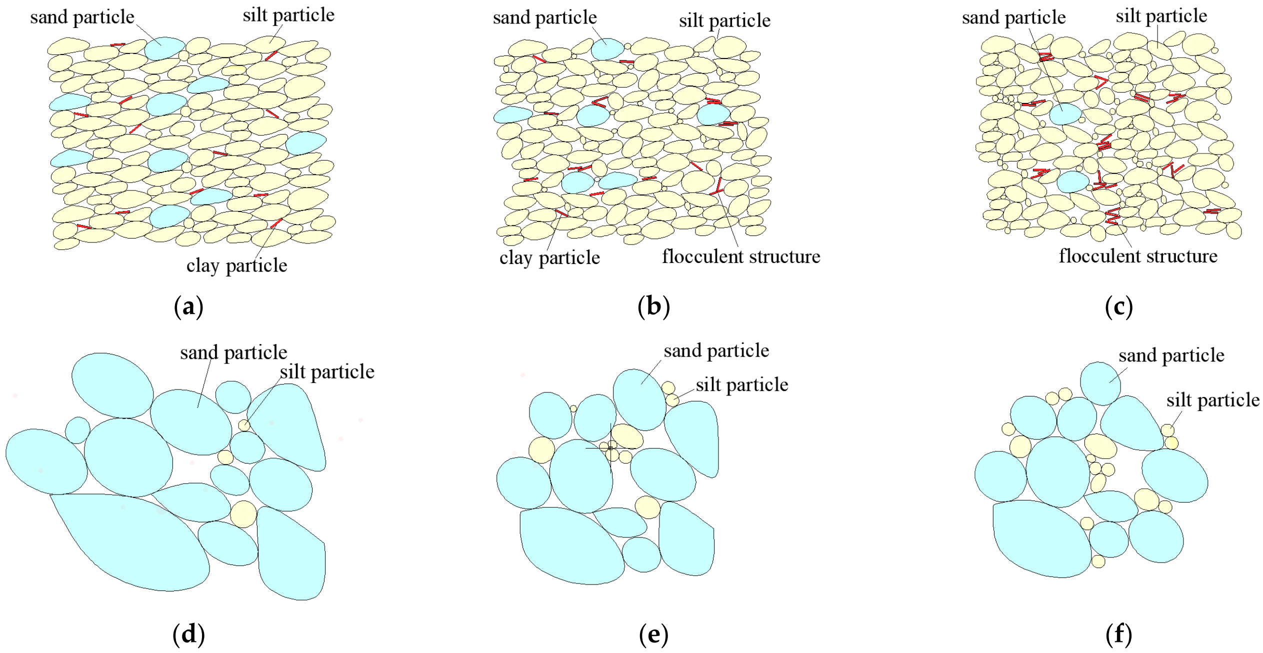

Figure 22. Schematic diagram of soil structure under freeze–thaw action. (**a**) Unfrozen silt; (**b**) silt after initial freeze–thaw cycle; (**c**) silt after long-term freeze–thaw cycles; (**d**) unfrozen sand; (**e**) sand after initial freeze–thaw cycle; (**f**) sand after long-term freeze–thaw cycles.

The content of clay particles in silty sand is very small, and total particle size is much larger than that of silt. Because of the small content of clay particles, SEM could not clearly observe the flocculent structure in silty sand after freeze–thaw, which only shows the characteristics of particle rearrangement and particle fragmentation (Figure 22e,f). The effects of freeze–thaw action on silt particles and sand particles in silty sand is similar to that in silt. Because the total particle size of silty sand is larger, the ability of individual particles to resist crushing deformation is stronger. Therefore, the effects of freeze–thaw action on silty sand is similar to that of silt, but the influence degree is smaller. The main distinction is the role of fine aggregate, especially for clay particles.

6. Conclusions

The SEM and LST tests were conducted to explore the effects of freeze–thaw action on the particle characteristics of saturated silt deposited in water environments. Several different impact factors were considered during sample reconstitution and freeze–thaw processes. The conclusions could be drawn as follows:

(1) Different for the only sand particle crushing in conventional soil shearing, freeze–thaw action could probably induce the particles' (60–200 μm) breakage, and also affect the clay particles' (less than 5 μm) aggregation and form flocculent structure. The diameters of flocculent structures and broken particles range from 5–60 μm. With continuous freeze–thaw cycles, this phenomenon could be more obvious. Freeze–thaw action could hardly influence the shape of particles smaller than 40 μm, and could

make the shape of particles larger than 40 μm more spherical (especially larger than 100 μm).

(2) Two parameters of particle size index and particle shape index are defined and specifically improved to quantitively evaluate the particle characteristics of silt under freeze–thaw action. They both hyperbolically increase with freeze–thaw cycles. Within 100 times, the influence degree of single freeze–thaw cycle on the particle size/shape of silt becomes smaller and gets more stable.

(3) Greater effective confining pressure, lower freezing temperature, greater compaction degree, and higher fine content could aggravate the influence of freeze–thaw cycles on particles' size and particles' shape for silt to a certain extent. From another aspect, the durability of pavements under freeze–thaw cycles could be comprehensively evaluated and controlled by these impact factors.

(4) From a perspective of freeze–thaw mechanism on different soil particles, two micro-structural evolution modes of particle characteristics under freeze–thaw action from initial freeze–thaw cycle to long-term freeze–thaw cycles have been inferred. The main distinction is the role of fine aggregate, especially for clay particles.

Author Contributions: Conceptualization, J.Z. and Z.L.; methodology, J.Z. and Z.L.; validation, J.Z. and W.P.; formal analysis, Z.L.; investigation, W.P.; resources, J.Z. and Z.L.; data curation, Z.L.; writing—original draft preparation, Z.L.; writing—review and editing, Z.L.; visualization, J.Z. and Z.L.; supervision, W.P.; project administration, J.Z.; funding acquisition, J.Z. All authors have read and agreed to the published version of the manuscript.

Funding: The research work herein was supported by National Natural Science Foundation of China (No. 41702299) and Foundation of State Key Laboratory of Frozen Soil Engineering (No. SKLFSE201916).

Conflicts of Interest: The authors declare no conflict of interest.

References

1. Arturo, E.C. The Frost Behavior of Soils. Part I: Vertical Sorting. In *Highway Research Board Bulletin*; U.S. Army Cold Regions Research and Engineering Laboratory: Hanover, NH, USA, 1962; pp. 9–34.
2. Arturo, E.C. The Frost Behavior of Soils: Laboratory and Field Data for a New Concept. Part II: Horizontal Sorting. In *Highway Research Board Bulletin*; U.S. Army Cold Regions Research and Engineering Laboratory: Hanover, NH, USA, 1962; pp. 46–64.
3. Edwin, J.C.; Anthony, J.G. Effect of freezing and thawing on the permeability and structure of soils. *Eng. Geol.* **1979**, *13*, 73–92.
4. Konrad, J.M. Physical processes during freeze-thaw cycles in clayey silts. *Cold Reg. Sci. Technol.* **1989**, *16*, 291–303. [CrossRef]
5. Qi, J.L.; Zhang, J.M.; Zhu, Y.L. The significance of soil mechanics of the effects of freezing and thawing on soil structure. *Chin. J. Rock Mech. Eng.* **2003**, *S2*, 2690–2694.
6. Mu, Y.H.; Ma, W.; Li, G.Y.; Mao, Y.C. Quantitative analysis of impacts of freeze-thaw cycles upon microstructure of compacted loess. *Chin. J. Geotech. Eng.* **2011**, *33*, 1919–1925.
7. Tan, Y.Z.; Wu, P.; Fu, W.; Wan Z, W.; Zhang, H.; Zhang, Z.H. Strength and micromechanism of improved silt under freeze-thaw cycle effect. *Rock Soil Mech.* **2013**, *34*, 2827–2834.
8. Tang, Y.Q.; Li, J.Z. Test method and application for microstructures of undisturbed silty sand and sandy silt. *Environ. Earth Sci.* **2018**, *77*, 657. [CrossRef]
9. Jin, Q.; Zheng, Y.J.; Cui, X.Z.; Cui, S.Q.; Qi, H.; Zhang, X.N.; Wang, S. Evaluation of dynamic characteristics of silt in Yellow River Flood Field after freeze-thaw cycles. *J. Cent. South Univ.* **2020**, *27*, 2113–2122. [CrossRef]
10. Zheng, Y.J.; Jin, Q.; Cui, X.Z.; Zhang, H.; Liu, Z.Q.; Zhang, J. Dynamic behavior and meso-damage evolution of saturated saline silt from yellow river flooded area under freeze-thaw cycle. *China J. Highw. Transp.* **2020**, *33*, 32–44.
11. Ren, J.; Vanapalli, S.K. Effect of freeze-thaw cycling on the soil-freezing characteristic curve of five Canadian soils. *Vadose Zone J.* **2020**, *19*, 1–8. [CrossRef]
12. Leuther, F.; Schlüter, S. Impact of freeze-thaw cycles on soil structure and soil hydraulic properties. *Soil* **2021**, *7*, 179–191. [CrossRef]
13. Zhou, J.; Li, Z.Y.; Tian, W.J.; Sun, J.W. Effects of Artificial Freezing on Liquefaction Characteristics of Nanjing Sand. *China Railw. Sci.* **2021**, *42*, 28–38.
14. Hardin, B.O. Crushing of soil particles. *J. Geotech. Eng.* **1985**, *111*, 1177–1192. [CrossRef]
15. Cavarretta, I.; Coop, M.R.; O'sullivan, C. The influence of particle characteristics on the behaviour of coarse grained soils. *Géotechnique* **2010**, *60*, 413–423. [CrossRef]
16. Marsal, R.J. Large-scale testing of rockfill materials. *ASCE J. Soil Mech. Found. Eng.* **1967**, *93*, 27–43. [CrossRef]

17. Zhang, S.; Tong, C.X.; Li, X.; Sheng, D. A new method for studying the evolution of particle breakage. *Géotechnique* **2015**, *65*, 911–922. [CrossRef]
18. Miller, R.D. Freezing and heaving of saturated and unsaturated soils. *Highw. Res. Rec.* **1972**, *399*, 1–11.
19. Christ, M.; Kim, Y.C. Experimental study on the physical-mechanical properties of frozen silt. *KSCE J. Civ. Eng.* **2009**, *13*, 317–324. [CrossRef]
20. Kim, S.Y.; Hong, W.T.; Lee, J.S. Silt fraction effects of frozen soils on frozen water content, strength, and stiffness. *Constr. Build. Mater.* **2018**, *183*, 565–577. [CrossRef]
21. Coop, M.R.; Sorensen, K.K.; Freitas, T.B.; Georgoutsos, G. Particle breakage during shearing of a carbonate sand. *Géotechnique* **2004**, *54*, 157–163. [CrossRef]
22. Fan, W.; Yang, P. Ground temperature characteristics during artificial freezing around a subway cross passage. *Transp. Geotech.* **2019**, *20*, 100250. [CrossRef]